JOURNAL OF CATALYSIS 111, 336–344 (1988)

Electronic Structures of $XMo_{12}O_{40}$ Heteropolyanions (X = P, As, Si, and Ge) and Their Reduction Behavior

KOICHI EGUCHI,* TETSURO SEIYAMA,* NOBORU YAMAZOE,* SINICHI KATSUKI,† AND HIROSHI TAKETA†

*Department of Materials Science and Technology, Graduate School of Engineering Sciences, Kyushu University 39, Kasugakoen, Kasuga-shi, Fukuoka 816, Japan; and †College of General Education, Kyushu University 01, Ropponmatsu, Fukuoka-shi, Fukuoka 812, Japan

Received January 27, 1986; revised January 4, 1988

Catalytic reduction and oxidation behavior were analyzed experimentally and theoretically for four isostructural heteropolyanions, $(PMo_{12}O_{40})^{3-}$, $(AsMo_{12}O_{40})^{3-}$, $(SiMo_{12}O_{40})^{4-}$, and $(GeMo_{12}O_{40})^{4-}$. The relative reducibility was determined as $(AsMo_{12}O_{40})^{3-} > (PMo_{12}O_{40})^{3-} > (GeMo_{12}O_{40})^{4-} > (SiMo_{12}O_{40})^{4-}$ by polarographic reduction. The catalytic activity for methacrolein oxidation was found to be $H_3PMo_{12}O_{40} > H_3AsMo_{12}O_{40} + H_3PMo_{12}O_{40} > H_4GeMo_{12}O_{40} > H_4SiMo_{12}O_{40}$. Theoretical calculations of the electronic structures by the $X\alpha$ model potential method for four heteropolyanions confirmed the catalytic reduction and oxidation behavior found by the experiments. The general features of the valence energy bands obtained by the calculations were all alike and not much affected by changing the central atom X (X = As, P, Ge, and Si). The highest occupied molecular orbitals (HOMO) were $13E$ and mostly composed of the oxygen atoms (O_b), bridging two molybdenum ions throughout the four anions. The result was consistent with a previous IR investigation which showed that the bridging oxygen species were exclusively active. The lowest unoccupied molecular orbitals (LUMO), except that for the As anion, were $14E$ and mostly composed of the Mo $4d$ orbitals and the O_b $2p$ orbitals and were antibonding with respect to the O_b–Mo bond. The LUMO for the As anion was $12A_1$ and mostly composed of As $4s$, O_{As} $2p$, and O_b $2p$ atomic orbitals. The $14E$ level was close in energy to the $12A_1$ level. The lower orbital energy of the LUMO, in general, is expected to cause the easier acceptance of the reduction electrons. Actually, the relative energies of the LUMO for the four anions in the present calculations were in accord with their relative reducibility. By the introduction of electrons into the LUMO of the heteropolyanions at the first stage of reduction, the bonds between O_b and MO were weakened and dissociated easily owing to the antibonding character of the LUMO with respect to the O_b–Mo bond. The selectivity to methacrylic acid was found to be related to the reducibility of the catalysts.

INTRODUCTION

Dodecamolybdophosphates are well known as oxidation and/or acid catalysts. Their structure is characterized by a large cluster anion which consists of 12 MoO_6 octahedra and a central PO_4 tetrahedron as shown in the coordination polyhedral model in Fig. 1. The heteropolyanions, which contain other Va and IVa elements, such as arsenic, silicon, and germanium in the central atom position, are known to be isostructural with the phosphorus analog (*1*) and can be isolated in the solid state as the acids and/or salts.

In our previous infrared spectroscopic experiments (*2*) on dodecamolybdophosphate, the oxygen atoms bridging two molybdenum ions have been revealed to be exclusively reactive and consumed in the early stage of reduction of the material. Although the four isostructural heteropolyanions have similar behavior in their catalytic reactions, the central atom difference is found to cause a slight difference in their chemical reactivity. Thus Tsigdinos (*3*) and Urabe *et al.* (*4*) reported from polarographic reduction experiments in aqueous solutions that the reducibility of the heteropolyanion was affected by the central atom species.

Catalytic oxidation reactions on these

0021-9517/88 $3.00

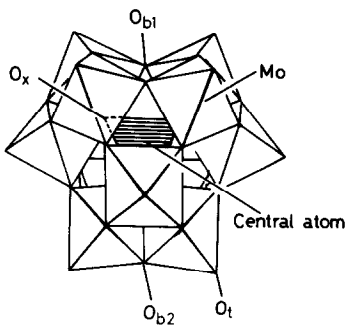

FIG. 1. Coordination polyhedral model of $(XMo_{12}O_{40})^{m-}$ anion. (X = P, As, Si, or Ge).

systems are believed to operate by a redox cycle of the heteropolyanion (*5*, *6*) which accompanies electron transfer between a reactant molecule and the heteropolyanion. Therefore, it is easily anticipated that the interactions between a reactant molecule and the polyanion must be strongly regulated by the electronic structure of the polyanion. From this point of view, we have calculated the electronic structure of dodecamolybdophosphate anion by the $X\alpha$ model potential method and reported the results in a preceding paper (*7*). The chemical reactivity upon reduction of the anion cluster turned out, as expected, to be well explained in terms of the highest occupied molecular orbital (HOMO) and the lowest unoccupied molecular orbital (LUMO). This success encouraged us to take the next step to calculate the electronic structures of the isostructural heteropolyanions containing P, As, Ge, or Si as the central atom and to elucidate the slight difference in chemical reactivity among them from the molecular orbital point of view. We believe this trial will help to throw light on the catalytic mechanism of these isostructural heteropolyanions.

EXPERIMENTAL AND THEORY

Procedure

The ease of reduction of the heteropolyanions was measured in water–dioxane solution by the polarographic method. The sample solution was prepared by mixing Na_2MoO_4 with Na_2HPO_4, Na_2HAsO_4, Na_2SiO_3, or Na_2GeO_3 (molar ratio = 12 : 1) in H_2O–dioxane solution (1 : 1) followed by acidification with sulfuric acid up to 0.5 *M* H_2SO_4 solution. The concentration of $(XMo_{12}O_{40})^{n-}$ in the resulting solution was 1.0×10^{-3} *M*. The acidified solution was used without further purification for a direct current polarogram. The potential of a rotating platinum cathode (1000 rpm) was controlled versus an Ag/AgCl reference electrode by a potentiostat connected to a function generator (Hokuto-Denko, HA-303). Nitrogen gas was fed to the solution before and during the measurement.

The solid acids, i.e., $H_3PMo_{12}O_{40}$, $H_4SiMo_{12}O_{40}$ (*8*), and $H_4GeMo_{12}O_{40}$ (*9*) were prepared according to the literature and calcined at 300°C. Their formation was confirmed by X-ray diffraction. Since pure molybdoarsenic acid is apt to decompose in an aqueous solution even in the presence of organic stabilizer, this sample was prepared as an equimolar mixture with molybdophosphoric acid. The formation of molybdoarsenate anion was confirmed by IR (*10*). Catalytic oxidation of methacrolein was tested in a flow system at 320°C according to a previously described method (*11*). A gaseous mixture of methacrolein (3.3%), O_2 (5.0%), and N_2 was fed to the catalyst at W/V = 2.0 g-cat sec/cm^3. The surface areas of catalysts were determined by the BET method.

Method of Calculation

The electronic structures of four isostructural anion clusters, i.e., $(PMo_{12}O_{40})^{3-}$, $(AsMo_{12}O_{40})^{3-}$, $(SiMo_{12}O_{40})^{4-}$, and $(GeMo_{12}O_{40})^{4-}$, were calculated by the $X\alpha$ method (*12*). The procedure was described in the preceding paper (*7*). Complete crystallographic analyses from X-ray diffraction studies were reported for $(SiMo_{12}O_{40})^{4-}$ (*13*) and $(GeMo_{12}O_{40})^{4-}$ (*14*) as well as for $(PMo_{12}O_{40})^{3-}$ (*15*, *16*). Although the $(AsMo_{12}O_{40})^{3-}$ cluster is also known to be isostructural with $(PMo_{12}O_{40})^{3-}$, the exact crystal

structure and atomic coordinates have not been reported yet as far as we know. Assuming the bonding lengths of As–O and Mo–O to be the same as those in the anion $(H_4As_4Mo_{12}O_{50})^{4-}$, which has a known structure (*17*), we constructed the isostructural polyanion. The atomic coordinates except those for $(PMo_{12}O_{40})^{3-}$ are slightly deviated from T_d symmetry. These systems are rather large and only a highly symmetric structure is within the reach of our manipulational ability in electronic structure calculations. Therefore, the coordinates of polyanions were averaged out to be T_d symmetric. The deviations from the T_d structure are small and the differences between the averaged-out bonding lengths and the experimentally obtained ones are within 3×10^{-3} nm. The resulting coordinates of the constituent atoms and the values of the radius of the Watson sphere, on which the stabilizing charges are distributed, are summarized in Table 1.

RESULTS AND DISCUSSION

Electrochemical Reduction of Polyanions

The electronic configuration of the unreduced heteropolyanion is described as $(X^{n+}Mo_{12}^{6+}O_{40})^{n-8}$ by assuming complete ionic bonding. This configuration changes with reduction, leading to the formation of Mo^{5+} ions as

$$(XMo^{6+}{}_{12}O_{40})^{m-} \xrightarrow{-y/2\ O} (XMo_{12-y}^{6+}Mo_y^{5+}O_{40-y/2})^{m-} \quad (1)$$
$$\xrightarrow[ye\ +\ yH^+]{} (XMo_{12-y}^{6+}Mo_y^{5+}O_{40}H_y)^{m-}$$

In order to measure the effect of the central atom on the reducibility of the polyanion, the four kinds of anions were reduced in aqueous solutions by a direct current polyarograms using a rotating Pt electrode. The reduction waves obtained are shown in Fig. 2. Every anion underwent reduction in several steps, each of which is attributed to the two-electron reduction of a polyanion according to Tsigdinos ($y = 2$ in Eq. (1)) (*3*).

The highest reduction potentials of the four anions are summarized in Table 2 together with reported values. Of the four samples, the reduction of $(AsMo_{12}O_{40})^{3-}$ anion began at the highest reduction potential. The experimentally obtained reducibilities of anions are

$$(AsMo_{12}O_{40})^{3-} > (PMo_{12}O_{40})^{3-} > (GeMo_{12}O_{40})^{4-} > (SiMo_{12}O_{40})^{4-}.$$

Effect of Central Atoms on Oxidation Catalysis

One of the most important applications of heteropolyanions as catalysts is the oxida-

TABLE 1

Atomic Coordinates (*A*) and Radius of Watson Sphere, r_w, for $(XMo_{12}O_{40})^{m-}$ Clusters (T_d Symmetry)

Atom	r_w = 5.931 Å		Atom	r_w = 5.819 Å	
	$x = y$	z		$x = y$	z
	$(PMo_{12}O_{40})^{3-}$			$(AsMo_{12}O_{40})^{3-}$	
P	0	0	As	0	0
Mo	2.519	0.100	Mo	2.475	0.112
O_P	0.890	0.890	O_{As}	0.976	0.976
O_{b1}	1.138	−2.979	O_{b1}	1.094	−2.908
O_{b2}	1.490	3.361	O_{b2}	1.586	3.550
O_t	3.688	−0.182	O_t	3.636	−0.245
Atom	r_w = 5.860 Å		Atom	r_w = 5.853 Å	
	$x = y$	z		$x = y$	z
	$(SiMo_{12}O_{40})^{4-}$			$(GeMo_{12}O_{40})^{4-}$	
Si	0	0	Ge	0	0
Mo	2.496	0.121	Mo	2.495	0.137
O_{Si}	0.940	0.940	O_{Ge}	0.999	0.999
O_{b1}	1.116	−2.945	O_{b1}	1.101	−2.936
O_{b2}	1.516	3.408	O_{b2}	1.531	3.427
O_t	3.650	−0.223	O_t	3.656	−0.219

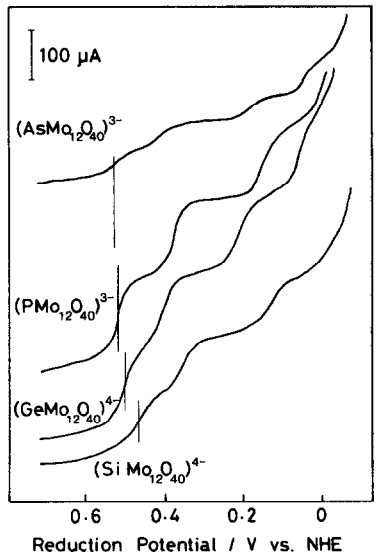

FIG. 2. Polarographic reduction wave of heteropolyanion. Anion (1×10^{-3} *M*) in H_2O–dioxane (1 : 1) solution (0.5 *M* H_2SO_4).

tion of methacrolein to methacrylic acid. As mentioned earlier, the catalysis involves a redox process. In this section, we investigate how the reducibility of the anion is reflected on the surface reaction using the four heteropoly acid samples as catalysts for oxidation of methacrolein. The rate of methacrolein oxidation per unit surface area of catalyst and the selectivity to methacrylic acid in the steady state are plotted versus the experimentally obtained reducibility of the anions in Fig. 3. It is seen that molybdophosphoric acid with an intermediate reducibility shows the highest catalytic activity. A steady state of the catalytic oxidation is determined as a point where the rate of reduction of the catalyst is equal to that of reoxidation. The reduction rate should increase monotonically as the reducibility of the polyanion increases, while the reverse should be true for the reoxidation rate. Thus, it is inferred that in the volcano-shape profile of the rate of catalytic oxidation shown in Fig. 3, the rates at the left- and right-hand sides are limited by the rates of reduction and reoxidation of

TABLE 2

Reduction Potential of Heteropolyanions $(XMo_{12}O_{40})^{m-}$

Anion	Reduction potential, E_r/*V* vs NHE		
	This study	Urabe *et al.* (*4*)	Tsigdinos (*3*)
$(AsMo_{12}O_{40})^{3-}$	0.526	—	0.66
$(PMo_{12}O_{40})^{3-}$	0.518	0.51	0.55
$(GeMo_{12}O_{40})^{4-}$	0.492	0.49	—
$(SiMo_{12}O_{40})^{4-}$	0.475	0.45	0.53

polyanions, respectively. The observed decrease in overall activity for $H_3AsMo_{12}O_{40}$ + $H_3PMo_{12}O_{40}$ which has the highest reducibility seems to result from a decrease in reoxidation rate. The thermal stability of this sample has not been studied in detail; however, the sample after the catalytic reaction did not contain decomposition products as was observed by X-ray diffraction and was soluble in acidified water. Since the catalytic behavior of $H_3AsMo_{12}O_{40}$ +

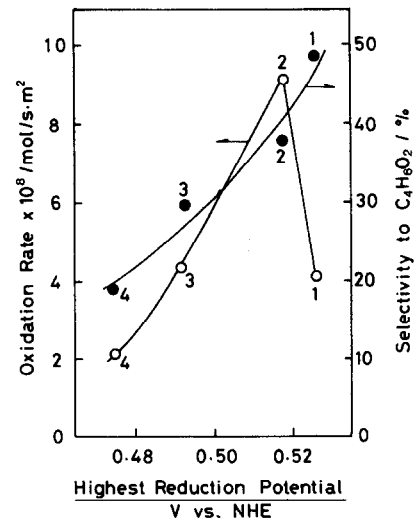

FIG. 3. Dependence of catalytic activity (○) and selectivity (●) on the reduction potential of the heteropolyanions. (1) $H_3AsMo_{12}O_{40}$ + $H_3PMo_{12}O_{40}$; (2) $H_3PMo_{12}O_{40}$ (3.9 m^2/g); (3) $H_4GeMo_{12}O_{40}$ (3.2 m^2/g); (4) $H_4SiMo_{12}O_{40}$ (10.6 m^2/g).

$H_3PM_{12}O_{40}$ is quite different from pure $H_3PMo_{12}O_{40}$, the anion structure appears to be maintained during the reaction. It should be noted that the selectivity to methacrylic acid is correlated monotonically with the reducibility of the anions, as shown in Fig. 3. The most reducible $H_3AsMo_{12}O_{40}$ + $H_3PMo_{12}O_{40}$ showed the highest methacrylic acid selectivity while that for $H_4SiMo_{12}O_{40}$ is the lowest. This suggests that the reduced surface is effective for producing methacrylic acid selectively.

Valence Energy Level Diagrams of $(XMo_{12}O_{40})^{m-}$ Anions

The valence-band electronic structures were calculated for the four anion clusters by the $X\alpha$ method to elucidate the central atom dependence of reduction and oxidation activity of the heteropolyanions from the molecular orbital point of view. The calculated valence energy levels of the four heteropolyanion clusters classified into six bands, group (1) through group (6), are shown in Fig. 4. Each level is expressed in electron volt units with reference to the vacuum level. The general features of the valence electronic structures of the four clusters are similar. There are 320 electrons in every cluster and 67 distinct orbitals are occupied by electrons and 32 orbitals are unoccupied virtual orbitals. The highest occupied molecular orbital (HOMO) is the top level of group (5) and the lowest unoccupied molecular orbital (LUMO) is the bottom level of group (6), throughout the four clusters. In the following explanations 40 oxygen atoms will be classified into four types, O_X, O_{b1}, O_{b2}, and O_t according to their bonding types in the cluster as shown in Fig. 1, because the bonding types of the lattice oxygen are expected to be responsible for the redox cycle of the polyanions.

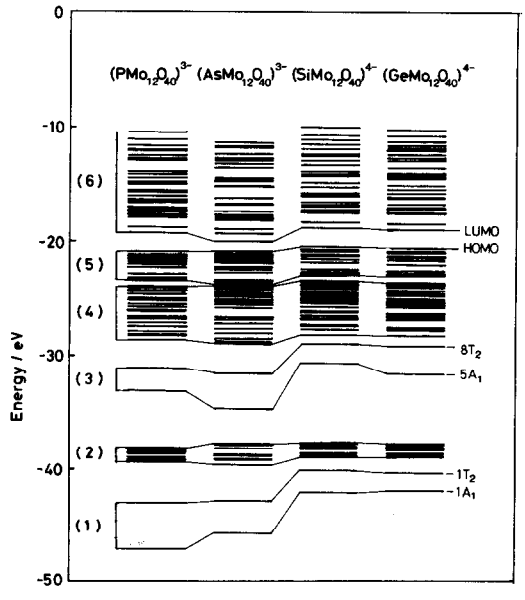

FIG. 4. Valence energy levels of $(XMo_{12}O_{40})^{m-}$.

The lowest two levels in the valence band belonging to group (1) of each cluster consist of s and p components of the central atom, X, and $2s$ and $2p$ components of O_X, by which the covalent X–O_X bonding is mainly constituted. Thirty-six pairs of electrons in group (2) are occupying 15 levels composed of $2s$ orbitals centered at 24 O_b atoms and 12 O_t atoms and scarcely contribute to metal–oxygen bonding. Two levels in group (3) consist of s and p components of the central atom X and $2s$ and $2p$ components of O_X. The relative magnitudes of the contributions to the X–O_X bond from the molecular orbitals in groups (1) and (3) are strongly dependent on the central atom. Of the six groups in all four clusters, the orbital energies in groups (1) and (3) are the most sensitive to the central atom, since these levels consist of a large component of orbitals centered on the central atom, and the molecular orbital energies are linked closely with the atomic valence energies. The energies of the levels for the two Va (P and As) clusters are relatively lower than those for the IVa (Si and Ge) clusters as summarized in Table 3.

Twenty-nine distinct levels in group (4) are bonding orbitals of Mo $4d$ and O $2p$ orbitals and 72 pairs of electrons occupying these levels contribute to the bondings between molybdenum atoms and oxygen atoms in the coordination frameworks of 12

TABLE 3

Energy of X–O_X Orbital and Atomic energy of X

Anion	Orbital energy (eV)				Energy of X in atomic state (eV)	
	$1A_1$	$1T_2$	$5A_1$	$8T_2$	s	p
$(PMo_{12}O_{40})^{3-}$	−47.05	−42.97	−33.11	−31.11	−12.82	−4.56
$(AsMo_{12}O_{40})^{3-}$	−45.60	−42.76	−34.65	−31.43	−13.13	−4.35
$(SiMo_{12}O_{40})^{4-}$	−42.01	−40.08	−30.61	−28.92	−9.80	−3.23
$(GeMo_{12}O_{40})^{4-}$	−41.78	−40.24	−31.51	−29.03	−10.55	−3.14

sets of MoO_6 octahedra. The molecular orbitals in group (5), which constitute the highest part of the occupied orbitals, consist of almost pure $2p$ components of the bridging oxygens and the terminal oxygens. These levels scarcely contain a metal component and can be regarded as main contributors to ionic bonding between Mo and O. The lowest part of the virtual band (group (6)) consists of levels containing antibonding Mo $4d$ and O $2p$ components with respect to Mo–O bonding. Since these orbitals are the lowest unoccupied molecular orbitals, they are good candidates for the electron acceptors in the reduction process of heteropolyanions. In the upper part of group (6), there are also two other kinds of levels, i.e., antibonding orbitals which include the X atom and O_X atom components and orbitals with the nearly pure Mo $5s$ component.

As mentioned above, each group has well-defined character and is clearly separated from others. This is in contrast to the calculations for smaller Mo clusters (*19, 20*). The calculations for larger clusters should give more realistic electronic structures of these materials.

Chemical Reactivity of Clusters from the MO Point of View

The present electronic structure calculations for 320 valence electron systems correspond to the fully oxidized form of the heteropolyanions. The reduction process as well as the reduced states of the polyanions were investigated experimentally by several researchers. Our previous infrared spectroscopic study on reduced dodecamolybdophosphates (*2*) revealed that not the terminal oxygen atoms but the bridging oxygen atoms are exclusively reactive and consumed in the early stage of the reduction process. The characteristics of the reduction and oxidation behavior were well understood in terms of HOMO and LUMO, as previously reported for the $(PMo_{12}O_{40})^{3-}$ cluster. According to the calculation, most of the HOMO (94%) was composed of the atomic $2p$ orbitals of the bridging oxygen. This result is consistent with the experimental findings that O_b sites serve as adsorption sites of a reactant molecule. The LUMO is a mixture of the Mo $4d$ orbitals (51%) and the O_b $2p$ orbitals (48%) and is antibonding with respect to the O_b–Mo bond according to the previous electronic calculation. This is also consistent with the experimental result that the O_b is exclusively consumed at the early stage of the reduction, because the bond between O_b and Mo should be weakened by the introduction of reduction electrons into the antibonding LUMO. The similarity seen in the general features of the energy diagram (Fig. 2) suggests that the characteristics of redox behavior will be common in the four heteropolyanions. The reason why the large components of the oxygens in the HOMO and the LUMO are from the bridging sites was

already analyzed in the preceding paper and can be applied throughout all four clusters. The subtle difference, however, will be caused by the different central atom species. We shall study this point in more detail in the following.

Effect of Central Atom on HOMO and LUMO

The electron density distributions of HOMO and LUMO by Mulliken's population analysis are summarized in Table 4, together with their orbital energies. The second highest virtual orbital for the As cluster is also included in Table 4 for comparison. The HOMO is the 13*E* orbital, consisting of an almost pure 2*p* component of bridging oxygen throughout the four anions. The composition ratio of O_{b1} and O_{b2} for the As anion, however, is slightly different from those for the other anions as shown in Table 4. This suggests that the relative activity of O_{b1} and O_{b2} is slightly dependent on the central atom species, although O_b site activities are similar.

Since the antibonding orbital of Mo–O_b, 14*E*, is the lowest occupied MO in the clusters of $(PMo_{12}O_{40})^{3-}$, $(SiMo_{12}O_{40})^{4-}$, and $(GeMo_{12}O_{40})^{4-}$, the introduction of electrons inevitably leads to weakening of the Mo–O_b bond. The LUMO for the $(AsMo_{12}O_{40})^{3-}$ cluster is $12A_1$, which consists of As 4*s*, O_{As} 2*p*, and O_{b2} 2*p* orbitals. The 14*E* orbital of the As anion is located next to the $12A_1$ orbital. The anion structure of reduced molybdoarsenate is expected to be unstable, because of the antibonding character of the $12A_1$ orbital with respect to As–O_{As} bonding. Of the four anions investigated, the $(AsMo_{12}O_{40})^{3-}$ anion was exceptionally unstable and easily changed into its component oxides.

The difference in reducibility is an important factor for the redox properties of oxidation catalysts. As already stated, the LUMO is very responsible for reduction of anions and oxidation of reactant molecules. The position of the LUMO, therefore, is expected to influence the reducibility of the anions. The most characteristic difference in the orbital energy diagram is that the orbital levels of anions with Va central atoms

TABLE 4

Orbital Energies and Mulliken Population Analysis of HOMO and LUMO for $(XMo_{12}O_{40})^{m-}$ Clusters

Anion	Orbital	Energy[a] (eV)	Mulliken population analysis[b]				
			Mo 4*d*	O_X 2*p*	O_{b1} 2*p*	O_{b2} 2*p*	O_t 2*p*
		Highest occupied MO					
$(PMo_{12}O_{40})^{3-}$	13*E*	−20.89	0.00	0.00	0.43	0.51	0.04
$(AsMo_{12}O_{40})^{3-}$	13*E*	−20.83	0.02	0.00	0.34	0.61	0.02
$(SiMo_{12}O_{40})^{4-}$	13*E*	−20.41	0.01	0.00	0.42	0.52	0.04
$(GeMo_{12}O_{40})^{4-}$	13*E*	−20.51	0.01	0.01	0.42	0.50	0.06
		Lowest unoccupied MO					
$(PMo_{12}O_{40})^{3-}$	14*E*	−19.29	0.50	0.00	0.21	0.27	0.00
$(AsMo_{12}O_{40})^{3-}$	$12A_1$	−19.99	0.03	0.35	0.23	0.23	0.06
$(SiMo_{12}O_{40})^{4-}$	14*E*	−18.78	0.50	0.00	0.27	0.27	0.06
$(GeMo_{12}O_{40})^{4-}$	14*E*	−18.86	0.49	0.00	0.27	0.27	0.06
$(AsMo_{12}O_{40})^{3-}$	14*E*	−19.29	0.48	0.00	0.19	0.32	0.00

[a] Orbital energy with reference to the vacuum level.
[b] Sum of values for equivalent atoms.

in general are located at a lower position than those with IVa atoms. Although the differences in orbital energies of groups (5) and (6) are not so obvious as those of groups (1) and (3) which are directly affected by the atomic orbital energies of the central atom, the central atom species are surely reflected in them through the X–O_X–Mo–O bonding chain. The calculated energy values of the LUMO for the four clusters range between 18 and 20 eV below the vacuum level as listed in Table 4 and are located in the sequence

$$(AsMo_{12}O_{40})^{3-} < (PMo_{12}O_{40})^{3-} < (GeMo_{12}O_{40})^{4-} < (SiMo_{12}O_{40})^{4-}$$

which suggests that the As anion is the most easily reducible and that the Si anion is the lowest in reducibility. This sequence is in quite good agreement with that obtained experimentally. The energy level of the LUMO is so sensitive to various factors that a conclusive explanation about the sequence cannot be made from the present results. The difference in reducibility between anions with IVa and Va atoms appears to be due to the larger formal charge of As^{5+} and P^{5+} than that of Si^{4+} and Ge^{4+}. A large positive charge may well attract an electron cloud from molybdenum, resulting in a low electronic energy. In addition to the electrostatic influence of the central atom, structural factors, such as Mo–O distances, are also important for the small energy differences between the clusters. It is interesting to note that the bonding length of Mo–O_b in the four anions tends to increase as the anion becomes more reducible.

CONCLUSIONS

The chemical reactivities of the four heteropolyanions are well explained in terms of the HOMO and the LUMO based on the electronic structures calculated for the four anion clusters in the present study. The general features for the valence electronic structures are not largely different because these anions are isostructural and their atomic coordinates in the Mo octahedra do not differ much. Electron density distributions of the HOMO and the LUMO corroborated the exclusively high reactivity of the bridging oxygens throughout the four clusters.

The central atom reflected a subtle difference in the catalytic reduction and oxidation behavior. The relative reducibility found by experiment could be explained by the sequence of the energy level locations of the LUMO with reference to the vacuum level obtained by the calculations. Catalytic oxidation of methacrolein is thus proved to be one of the good examples where chemical reactivities of clusters are strongly regulated by their electronic structures. The reason is that this reaction is operated by a redox cycle of the polyanions and electron transfer between polyanions and reactant molecules plays a leading role.

From the present study, it can be concluded that an electronic structure calculation is quite effective in clarifying the mechanism of chemical reactions which involve electron transfer between catalyst and reactants. At the same time the $X\alpha$ model potential method is well suited to the calculation of the electronic structure of the four rather complicated systems studied here.

ACKNOWLEDGMENTS

The numerical computations were made with the FACOM M382 computing facility of Kyushu University and the HITAC M200 computing facility of the Institute for Molecular Science. The present work was supported in part by the Grant-in-Aid for Scientific Research from the Ministry of Education.

REFERENCES

1. Tsigdinos, G. A., *Top. Curr. Chem.* **76,** 1 (1978).
2. Eguchi, K., Toyozawa, Y., Yamazoe, N., and Seiyama, T., *J. Catal.* **83,** 32 (1983).
3. Tsigdinos, G. A., "Climax Molybdenum Bulletin, Cdb 15." Climax Molybdenum Co., 1971.
4. Urabe, K., Fujii, Y., Kimura, F., and Izumi, Y., *Shokubai* (*Catalyst*) **23,** 290 (1981).
5. Tsuneki, H., Niiyama, H., and Echigoya, E., *Chem. Lett.*, 1183 (1978).
6. Misono, M., Sakata, K., Yoneda, Y., and Lee, W. Y., "Proceedings, 7th International Congress on Catalysis, Tokyo, 1980" Kodansha/Elsevier (T.

Seiyama and K. Tanabe, Eds.), p. 1047. Tokyo/Amsterdam, 1981.
7. Taketa, H., Katsuki, S., Eguchi, K., Yamazoe, N., and Seiyama, T., *J. Phys. Chem.* **90,** 2959 (1986).
8. Tsigdinos, G. A., *Ind. Eng. Chem. Prod. Res. Dev.* **13,** 267 (1974).
9. Grosscup, C. G., *J. Amer. Chem. Soc.* **52,** 5154.
10. Rocchiccioli-Deltcheff, C., Thouvenot, R., and Frank, R., *Spectrochim. Acta A* **32,** 587 (1976).
11. Eguchi, K., Aso, I., Yamazoe, N., and Seiyama, T., *Chem. Lett.,* 1345 (1979).
12. Katsuki, S., and Inokuchi, M., *J. Phys. Soc. Japan* **51,** 3652 (1982).
13. Feist, M., Molchanov, V. N., Kazanskii, L. P., Torchenkova, E. A., Spitsyn, V. I., *Z. Neorg. Khim.* **25,** 733 (1980).
14. Strandberg, R., *Acta Crystallogr. B* **33,** 3090 (1977).
15. Strandberg, R., *Acta Chem. Scand. A* **29,** 359 (1975).
16. Allmann, R., *Acta Chem. Scand. A* **30,** 152 (1976).
17. Nishikawa, T., Sasaki, Y., *Chem. Lett.,* 1185 (1975).
18. Broclawik, E., Foti, A. E., and Smith, V. H., *J. Catal.* **51,** 380 (1978).
19. Broclawik, E., Foti, A. E., and Smith, V. H., *J. Catal.* **67,** 103 (1981).